A Thieno[2,3-b]pyridine-Flanked Diketopyrrolopyrrole Polymer as an n-Type Polymer Semiconductor for All-Polymer Solar Cells and Organic Field-Effect Transistors

A thieno[2,3-*b*]pyridine-flanked diketopyrrolopyrrole polymer as an n-type polymer semiconductor for all-polymer solar cells and organic field-effect transistors

Hung-Yang Chen,[*,†] *Mark Nikolka,*[‡] *Andrew Wadsworth,*[†] *Wan Yue,*[†,∥] *Ada Onwubiko*,[†] *Mingfei Xiao,*[‡] *Andrew J. P. White,*[†] *Derya Baran,*[†,§] *Henning Sirringhaus*[‡] *and Iain McCulloch*[†,§]

[†]Department of Chemistry and Centre for Plastic Electronics, Imperial College London, London, SW7 2AZ, UK.

[‡]Cavendish Laboratory, University of Cambridge, J. J. Thompson avenue, Cambridge, CB3 0HE, UK.

[§]King Abdullah University of Science and Technology (KAUST), KSC, Thuwal, 23955-6900, Saudi Arabia.

[∥]Key Laboratory for Polymeric Composite and Functional Materials of Ministry of Education, School of Material and Material Engineering, Sun Yat-Sen University, Guangzhou 510275, China.

Keywords: Diketopyrrolopyrrole (DPP), polymer acceptor, all polymer solar cells, n-type OFETs.

ABSTRACT A novel fused heterocycle-flanked diketopyrrolopyrrole (DPP) monomer, thieno[2,3-*b*]pyridine diketopyrrolopyrrole (TPDPP), was designed and synthesized. When copolymerized with 3,4-difluorothiophene using Stille coupling polymerization, the new polymer pTPDPP-TF possesses a highly planar conjugated polymer backbone due to the fused thieno[2,3-*b*]pyridine flanking unit that effectively alleviates the steric hindrance both with the central DPP core as well as the 3,4-difluorothiophene repeat unit. This new polymer exhibits a high electron affinity (EA) of -4.1 eV and was successfully utilized as an n-type polymer semiconductor for applications in organic field-effect transistors (OFETs) and all polymer solar cells. A promising n-type charge carrier mobility of 0.1 $cm^2V^{-1}s^{-1}$ was obtained in bottom-contact, top-gate OFETs and power conversion efficiency (PCE) of 2.72 % with a high open-circuit voltage (V_{OC}) of 1.04 V was achieved for all polymer solar cells using PTB7-Th as the polymer donor.

INTRODUCTION Solution-processable polymer semiconductors are promising candidates to realize next-generation lightweight and flexible electronics, such as organic field-effect transistors (OFETs) and organic solar cells (OSCs), via low cost and large area printing. The last decade has witnessed a tremendous advance in p-type polymer semiconductors with hole mobilities surpassing 10 $cm^2V^{-1}s^{-1}$ in OFETs[1,2] and power conversion efficiencies (PCEs) above 11% in OSCs.[3,4] To achieve broad applications of organic electronics such as organic complementary circuits and all polymer solar cells, congruent performances for both p- and n-type polymer semiconductors are desired. However, the progress in n-type polymer semiconductor development is much slower in comparison with its p-type counterparts with few polymers demonstrating

electron mobility higher than 5 $cm^2V^{-1}s^{-1}$ in OFETs[5,6] and PCEs higher than 7% as acceptors in OSCs.[7-11] Moreover, most high performance n-type polymer semiconductors are constructed by rylene diimide-based structure, such as perylene diimide (PDI),[11-13] naphthalene diimide (NDI),[8,10,14] or naphthodithiophene diimide (NDTI).[15,16]

Diketopyrrolopyrrole (DPP)–based small molecules and polymers have shown excellent performance as p-type semiconductors in OFETs and OSCs[17] due to their high structural planarity, small optical gap,[18] and high absorption coefficient.[19] Impressive hole mobility of higher than 1 $cm^2V^{-1}s^{-1}$ in OFETs[20,21] and PCEs above 8% as donors in OSCs[20,22] have been reported in these DPP polymers. High short-circuit current (J_{SC}) of larger than 20 $mAcm^{-2}$ in OSCs using DPP polymer donors are also reported.[20,23] The bicyclic DPP core is usually flanked with electron-rich aryl units on both sides at the 3 and 6 positions of DPP; such as phenyl, furan, thiophene, selenophene, and thieno[3,2-*b*]thiophene.[18,24,25] Although the bis-lactam core DPP unit is electron-deficient, few examples are demonstrated to realize DPP-based polymers as predominantly n-type polymer semiconductors.[26] These examples utilize electron-deficient comonomers, such as benzothiadiazole,[27] fluorinated phenylene,[28] and thienyl-cyanovinylene,[29] to increase the electron affinity (EA) and achieve n-type charge transport.

There are, however, very few examples reported with modification by electron-deficient flanking substituents on the DPP core. Replacement of thiophene by thiazole to synthesize a thiazole-flanked DPP unit was successfully employed as a building block for n-type polymer semiconductors. The polymer PDPP2TzT possesses an electron mobility of 0.13 $cm^2V^{-1}s^{-1}$ in OFET and was employed as an acceptor in OSC with a PCE around 3%.[30,31] Pyridine was also chosen as the flanking substituent for the DPP core, which is more electron deficient than the commonly used aryl units (thiophene, furan, and benzene) and also possesses a smaller steric

hindrance between the N-CH_2 of the alkyl chain and the nitrogen atom at the ortho-position of pyridine.[5] When copolymerized with 2,2'-bithiophene, the polymer PDBPyBT demonstrated ambipolar charge transport compared with its analogous thiophene polymer, PDQT, which showed only p-type charge transport.[32]

A DPP-based repeat unit bearing the fused heterocycle, thieno[3,2-*b*]thiophene, has previously been demonstrated with impressive performances as p-type semiconducting polymers in both OFETs and OSCs.[20,25,33,34] The fused heterocycle substituent with increased intermolecular association through extended polymer coplanarity was shown to enhance intermolecular charge-carrier hopping. This approach was used to design an n-type semiconducting polymer based on the DPP core with electron deficient flanking unit. A fused heterocycle thieno[2,3-*b*]pyridine was chosen as the flanking unit (Scheme 1). Thieno[3,2-*b*]thiophene-flanked DPP unit has less steric effects than phenyl flanked units as the five-membered ring of thiophene adjacent to the DPP core does not possess alpha C-H groups which can exhibit torsional twisting, thus increasing the dihedral angle between the linked units. On the other hand, thieno[2,3-*b*]pyridine-flanked DPP monomer also shows a suppressed steric hindrance through the positioning of the less steric nitrogen atom adjacent to the DPP core to improve the co-planarity. Furthermore, thieno[2,3-*b*]pyridine is more electron deficient than thieno[3,2-*b*]thiophene which has the benefit of increasing the electron affinity. Besides, we choose thieno[2,3-*b*]pyridine as the flanking substituent rather than thieno[3,2-*b*]pyridine is due to its ability to adopt a quinoid resonance form, which is potential for smaller band gap and better charge transport for the polymer chain. However, a quinoid resonance structure cannot be formed when using thieno[3,2-*b*]pyridine as the flanking substituent on the DPP core. Additionally, compared with the pyridine-flanked DPP polymer, PDBPyBT, which has a larger steric hindrance between 3,5-positions of hydrogen atoms on the

pyridine with linking co-monomers, the flanking thiophene on the thieno[2,3-*b*]pyridine flanked DPP should have reduced backbone twisting with linking co-monomers compared with the pyridine-flanked DPP monomer.[5] As shown in Scheme 1, the electron-deficient 3,4-difluorothiophene was chosen as the co-monomer to ensure a high co-planarity and high electron affinity (EA) for the polymer.

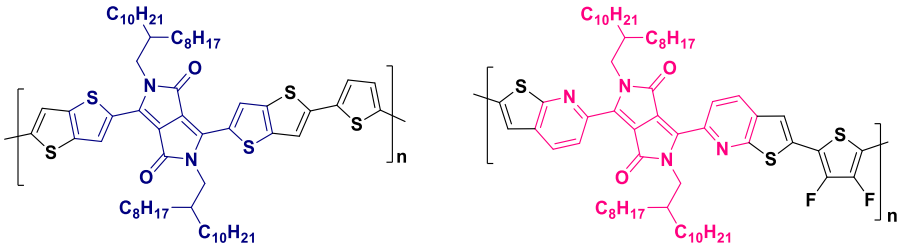

Scheme 1. Fused heterocycle-flanked DPP polymers.

RESULTS AND DISCUSSION

Scheme 2 shows the synthetic routes of the brominated thieno[2,3-*b*]pyridine-diketopyrrolopyrrole (TPDPP) monomer and its derivatives. Initially, the thieno[2,3-*b*]pyridine core was synthesized in one step from commercially available 2-nitrothiophene according to the literature procedure.[35] Beyond our expectations, it was tortuous to obtain the TPDPP monomer. Firstly, we started our approach using route I following reactions analogous to those commonly used in the diaryl-DPP. The carbonitrile precursor in preparing DPP, thieno[2,3-*b*]pyridine-6-carbonitrile 3, can be easily synthesized from thieno[2,3-*b*]pyridine by two steps in moderate yields. After obtaining the non-alkylated TPDPP 4 from 3 according the literature method, a long and branched 2-octyldodecyl chain was anchored on the TPDPP core to obtain C8C10-TPDPP to ensure a good solubility for the polymer. However, the bromination of C8C10-TPDPP using N-bromosuccinimde (NBS) or liquid bromine resulted in a decomposition of the TPDPP core and unidentified side products.

We therefore modified our synthetic route to introduce the bromine atom at the earlier step as presented in route II. Bromination of thieno[2,3-*b*]pyridine-6-carbonitrile 3 using N-bromosuccinimide proceeded smoothly in DMF. Surprisingly, it was found afterwards that the bromination occurred at the β-position of 3 to afford 5, with the consequence that the UV-Vis absorption spectrum of the polymer obtained from the β-position dibrominated TPDPP monomer, β-Br_2TPDPP, and distannylated thiophene by Stille polymerization having a much higher energy absorption than expected (see supporting information, Figure S7). As shown in Figure S7, the absorption of the polymer pTPDPP-β-T shows a less bathochromic shift compared with the monomer β-Br_2TPDPP, which is not in accordance with literature reported DPP polymers using thiophene as the co-monomer. This is likely due to cross conjugation and therefore reduced delocalisation. Therefore, a single crystal of 3-bromothieno[2,3-*b*]pyridine-6-carbonitrile 5 was prepared to confirm the position of the bromine atom on the thieno[2,3-*b*]pyridine-6-carbonitrile. The absolute configuration of the single-crystal structure indeed shows the bromination occurred at the β-position of 3 and crystal data of compound 5 are shown in the supporting information (Figure S4). A previous literature has also shown the bromination of thieno[2,3-*b*]pyridine[35] using liquid bromine can lead to the β-position brominated product. A similar situation also occured in the case of benzo[*b*]thiophene.[36] Due to the higher reactivity for the β-position of thieno[2,3-*b*]pyridine-6-carbonitrile 3 under electrophilic halogenation, we changed our strategy by using *n*-butyl lithium to deprotonate the α-position of thieno[2,3-*b*]pyridine 1. The nucleophilic α-lithiated thieno[2,3-*b*]pyridine was then reacted with the bromine source tetrabromomethane (CBr_4) to afford 2-bromothieno[2,3-*b*]pyridine 7. The carbonitrile precursor, 2-bromothieno[2,3-*b*]pyridine-6-carbonitrile 9, was obtained in two steps analogous to those in Route I, in which the structure of compound 9 was also confirmed from its single crystal (Figure S5). Finally, the α-position

dibrominated TPDPP, α-Br_2TPDPP, was obtained from 9 as a deep red solid, which is soluble in common organic solvents.

As shown in Scheme 3, the polymer pTPDPP-TF was then synthesized from dibrominated TPDPP monomer, α-Br_2TPDPP, and 2,5-bis(trimethylstannyl)-3,4-difluorothiophene co-monomer using palladium-catalyzed Stille coupling polymerization. The crude polymer was purified by Soxhlet extraction in the sequence of methanol, hexane, ethyl acetate, and chloroform. The purified polymer, soluble in chloroform, chlorobenzene, and 1,2-dichlorobenzene at room temperature, has a weight average molecular weight (M_w) of 125.3 kDa and number average molecular weight (M_n) of 24.4 kDa giving a polydispersity (PDI) of 5.1, likely an overestimate due to aggregating effects in solution.

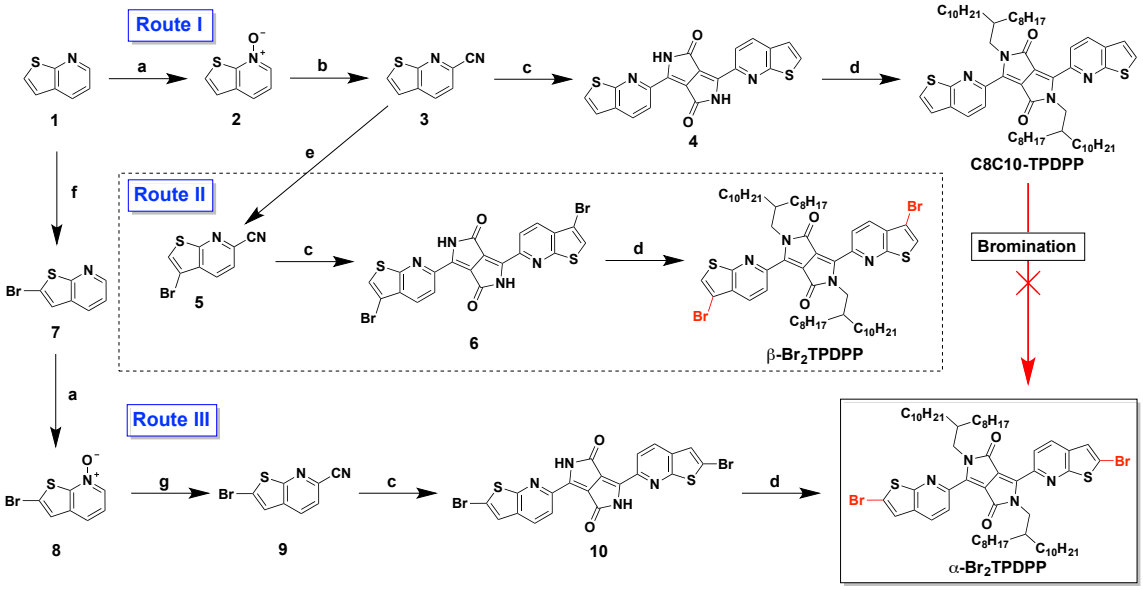

Scheme 2. Synthetic route of thieno[2,3-*b*]pyridine-diketopyrrolopyrrole (TPDPP) and brominated thieno[2,3-*b*]pyridine-diketopyrrolopyrrole (α- and β-brominated TPDPP). Reagents: (a) *m*-CPBA, $CHCl_3$; (b) dimethylcarbamyl chloride, trimethylsilyl cyanide, CH_3CN; (c) Na, cat. $FeCl_3$, 2-methyl-2-butanol, diethyl succinate; (d) 9-(bromomethyl)nonadecane, K_2CO_3, 18-crown-6, DMF; (e) NBS, DMF; (f) i. ^{n}BuLi / THF, ii. CBr_4 / THF; (g) dimethylcarbamyl chloride, trimethylsilyl cyanide, CH_2Cl_2.

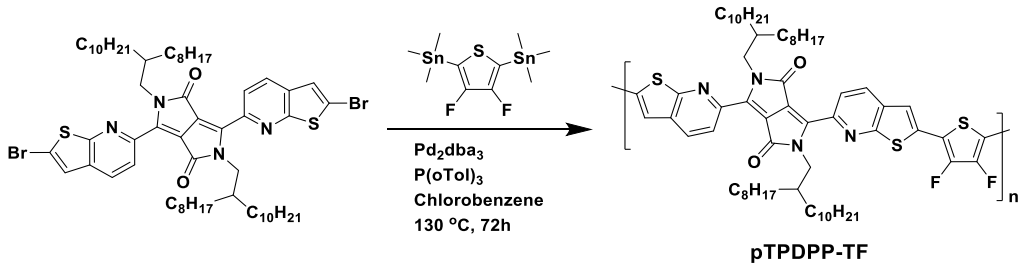

Scheme 3. Synthesis of pTPDPP-TF.

To confirm the planarity of the new TPDPP monomer, a model TPDPP small molecule anchored with two shorter 2-ethylhexyl branched chains (2EH-TPDPP) was synthesized, and the single crystal structure was easily obtained from slow evaporation of a binary solvent system (chloroform and methanol). Detailed crystallographic data are shown in Figure S6. Figure 1 shows the single crystal structure of 2EH-TPDPP, which exhibits a dihedral angle of 7.1° between the thieno[2,3-*b*]pyridine ring and the DPP core. Although 2-pyridinyl substituted DPP block has been reported with a dihedral angle between pyridine and the DPP core being 0° from computer simulations,[5] no applicable references of the pyridinyl-DPP crystal structure are available to the best of our knowledge. Moreover, the small dihedral angle of 2EH-TPDPP is similar to thiophene-containing DPP molecules that have dihedral angles ranging from 3° to 9° in several reported crystal structures.[37] This indicates that a highly coplanar structure and π-electron delocalization could be achieved in the polymer backbone when using TPDPP as the building block.

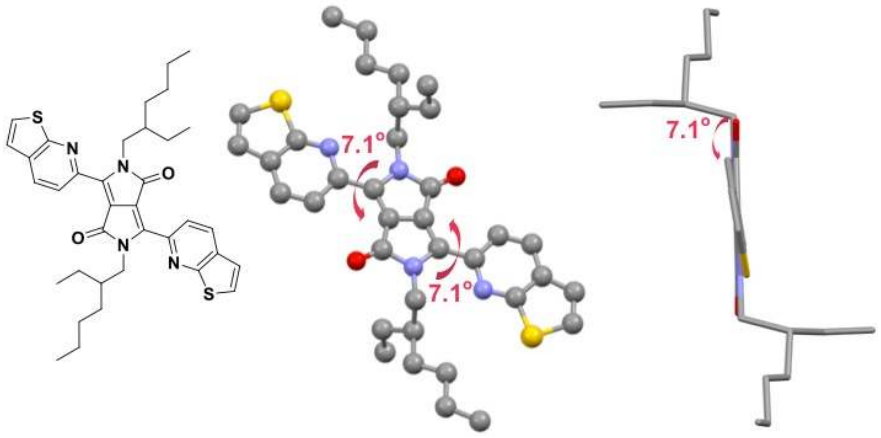

Figure 1. The chemical structure and single crystal structure (front and side view) of 2EH-TPDPP.

As shown in Figure 2, the UV-Vis absorption spectra of pTPDPP-TF in 1,2-dichlorobenzene (1,2-DCB) and as thin film exhibit almost the same absorption profile. This is attributed to small polymer aggregates of pTPDPP-TF in 1,2-DCB solution, showing two vibronic peaks at around 642 nm and 711 nm. The optical band gap calculated from the onset absorption of the thin film is 1.66 eV, which is significantly larger than the thieno[3,2-*b*]thiophene-flanked DPP polymer (1.38 eV).[25] This can be attributed to a lower degree of intramolecular donor-acceptor molecular orbital hybridisation among the polymer conjugation backbone of pTPDPP-TF.

Photoelectron spectroscopy in air (PESA) was utilized to measure the ionization potential (IP) of pTPDPP-TF thin films. A large IP of -5.8 eV was measured and the electron affinity (EA) was subsequently obtained as -4.1 eV by the addition of its optical band gap. The EA of pTPDPP-TF is significantly higher than that of thieno[3,2-*b*]thiophene-flanked DPP polymer (-3.7 eV).[25] This high EA value would be beneficial in electron injection for n-type OFETs and also to promote charge separation in donor/acceptor blends in bulk-heterojunction OSCs. In considering the ability of pTPDPP-TF to be utilized as an n-type semiconductor, cyclic voltammetry (CV) was used to study its electron affinity and the stability of its negatively charged polaron. As shown clearly in Figure 2, a reversible reduction cycle was observed, suggesting its excellent electron-accepting

ability and reversibility. The EA value of pTPDPP-TF calculated from the onset reduction potential is -3.51 eV, which is higher lying than that of $PC_{71}BM$ (-3.90 eV) measured in the same condition (see supporting information). An improved open-circuit voltage (V_{OC}) relative to $PC_{71}BM$ can be expected in the solar cell when using pTPDPP-TF as the acceptor.

pTPDPP-TF adopts a lamellar type packing motif similar with other DPP polymers,[18,20] which can be evident from the (100) and (200) diffraction peaks in its XRD diffractogram (Figure 2 Right). The first-order diffraction peak $2\theta = 4.5^{o}$ corresponds to a d-spacing of 19.7 Å. Although pTPDPP-TF orients predominantly edge-on relative to the substrate as evident from the stronger intensity of (100) diffraction peak, we assume the broad featureless diffractions from $2\theta = 15$ to 30^{o} likely contain reflections from face-on crystallites and other tilted chain orientations.[38]

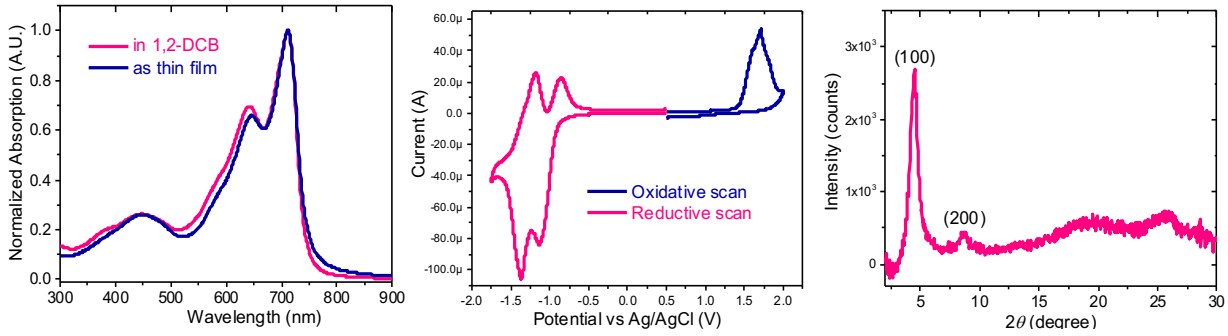

Figure 2. Left: Normalized UV-Vis absorption spectra of pTPDPP-TF in 1,2-dichlorobenzene and as thin film; Middle: cyclic voltammograms of pTPDPP-TF thin film drop cast on a Pt working electrode (reference electrode: Ag/AgCl, counter electrode: Pt gauze, electrolyte solution: 0.1M $TBAPF_6$ in anhydrous acetonitrile); Right: XRD diffractogram of the as cast film on Si wafer for pTPDPP-TF.

In order to further probe the dihedral angles between adjacent backbone units, a computational modelling study using density functional theory (DFT) at the B3LYP 6-31G level was used to predict energy-minimized polymer backbone structure and study backbone planarity for pTPDPP-TF. As shown in Figure 3, pTPDPP-TF exhibits close to coplanar dihedral angles between the DPP

unit and adjacent substituents (thieno[2,3-*b*]pyridine). This is attributed to the effective suppression of steric hindrance from the 2-pyridinyl groups. However, there is more of a twist in the molecule, as observed from the single crystal structure, than is predicted by DFT. It is possible that the small twist may arise from the longer alkyl chain (2-ethylhexyl) of the model compound than the calculated structure (methyl). Furthermore, pTPDPP-TF is almost completely co-planar along the backbone due to the absence of steric hindrance between TPDPP monomer and 3,4-difluorothiophene monomers. This highly planar polymer backbone is in agreement with its tendency of forming small aggregates in solution due to strong π-π interactions between polymer chains.

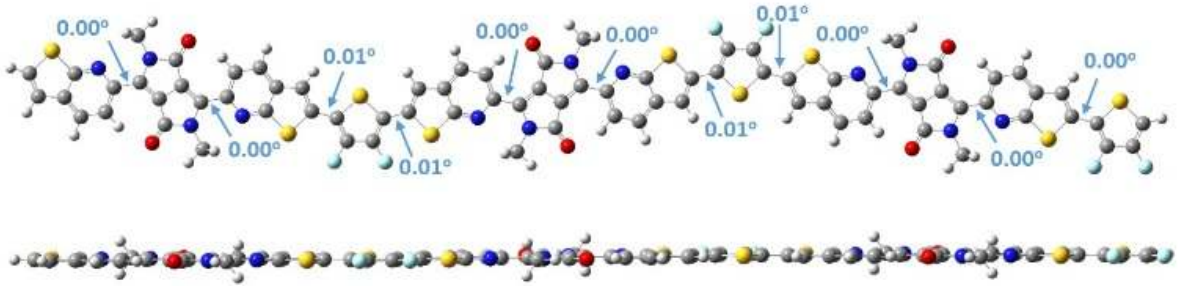

Figure 3. Dihedral angels of energy-minimized polymer backbone structure of pTPDPP-TF (front and side view).

In Figure 4, representative transfer characteristics of OFET for the investigated polymer pTPDPP-TF are shown. We find that in our device architecture (bottom-contact, top-gate with gold electrodes), after annealing at 100 ºC, pTPDPP-TF exhibits ambipolar charge transport characteristics with more pronounced n-type than p-type transport behavior was observed. As evident from the gate-voltage (V_G) dependence of extracted charge carrier mobilities presented in Figure 4(a), we found that the maximum n-type field-effect mobility of pTPDPP-TF was obtained as 0.1 $cm^2V^{-1}s^{-1}$ with a corresponding on-off ratio of 10^4 and the threshold voltage for pTPDPP-TF

OFET was 14 V. Fitting of the transfer characteristics with an ideal MOSFET model as described elsewhere[39] results in a conservative mobility of 0.04 $cm^2V^{-1}s^{-1}$. The output characteristics in Figure 4(b) do not exhibit the typical s-shape associated with an injection barrier suggesting that the LUMO level is close enough to the electrode Fermi level to provide good injection of electrons.

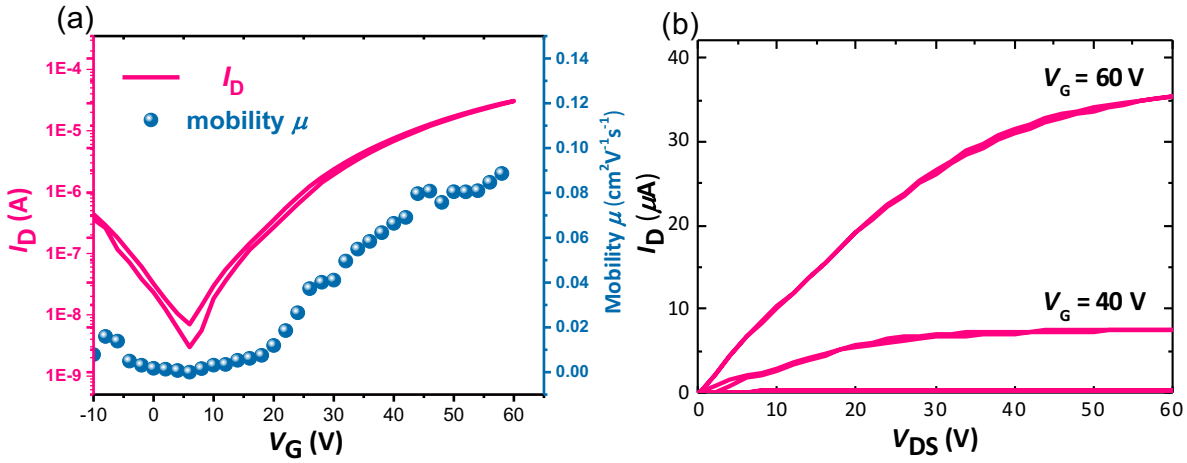

Figure 4. (a) Transistor transfer characteristics and gate-voltage (V_G) dependence of saturation mobility for OFETs (L = 20 μm, W = 1 mm); (b) N-type output characteristics for pTPDPP-TF gate-voltage (V_G).

Polymer-polymer solar cells, using PTB7-Th (also known as PBDTTT-EFT) as the donor and pTPDPP-TF as the acceptor, were fabricated in an inverted device architecture of glass/ITO/ZnO/PTB7-Th:pTPDPP-TF (1:1)/MoO_3/Ag. PTB7-Th has been reported to have an EA value of -3.66 eV and a IP value of -5.24 eV using ultraviolet photoelectron spectroscopy (UPS);[40] therefore, sufficient energetic offsets between PTB7-Th and pTPDPP-TF were expected for charge separation. The active layer solution was prepared in 1,2-dichlorobenzene, without the use of additives. The best device gave a power conversion efficiency (PCE) of 2.72 % with a short-circuit

current density (J_{SC}) of 6.57 mAcm^{-2}. A low fill factor (FF) of 0.40 was obtained, suggesting poor phase separation in the blend, resulting in significant charge recombination.[30] However, a high open-circuit voltage (V_{OC}) of 1.04 V was obtained, which has a significant improvement compared with the PCE10:$PC_{71}BM$ blend due to the higher EA of pTPDPP-TF (according to our comparison of EA values from cyclic voltammetry).[40] The EQE of the best PTB7-Th:pTPDPP-TF device is shown in Figure 6(b), alongside the normalized absorption spectra of pristine PTB7-Th and pTPDPP-TF. It can be seen clearly that the EQE around 450 nm is mainly contributed from pTPDPP-TF due to its stronger absorption in this spectral region. This is also evidence of charge generation from "channel II",[41] where the exciton was generated from the acceptor, followed by hole transfer from acceptor to donor. The EQE in the range of 500 to 800 nm can be attributed to both PTB7-Th and pTPDPP-TF, due to their overlapping absorptions and the stronger EQE intensity.

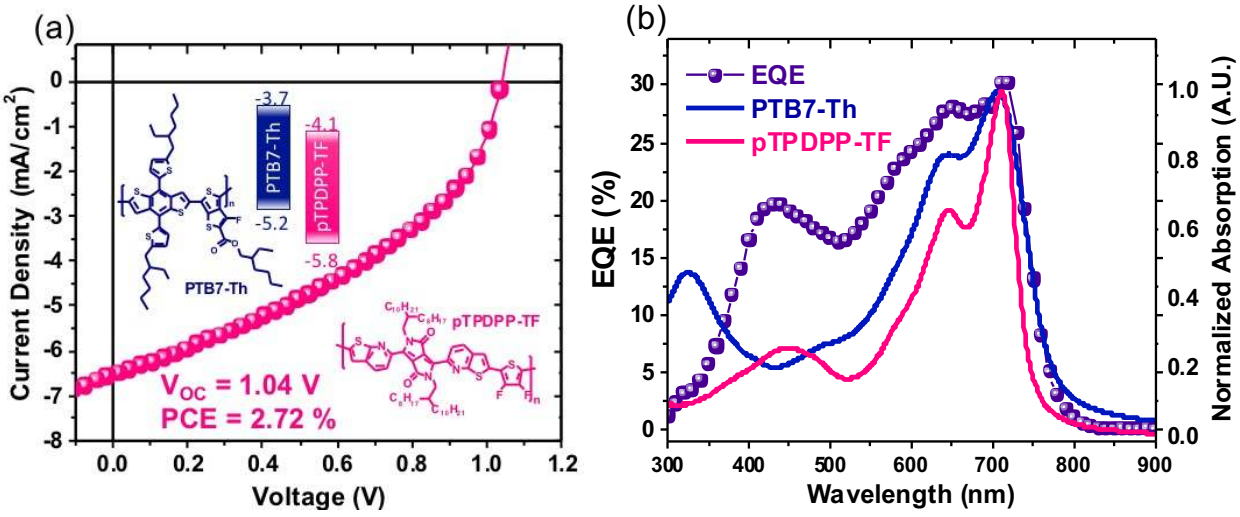

Figure 5. (a) *J-V* curves of optimized PTB7-Th:pTPDPP-TF (1:1) solar cell; (b) EQE spectrum (line+symbol) of optimized PTB7-Th:pTPDPP-TF (1:1) solar cell alongside normalized thin film absorption spectra (line) of PTB7-Th and pTPDPP-TF.

CONCLUSIONS A new fused heterocycle-flanked diketopyrrolopyrrole (DPP) monomer possessing a planar and electron-deficient structure was designed and successfully synthesized. The fused thieno[2,3-*b*]pyridine flanking unit effectively alleviates the steric hindrance both with the central DPP core and the co-monomers due to the less sterically nitrogen atom and thiophene ring on the thieno[2,3-*b*]pyridine, respectively. When copolymerized with electron-deficient 3,4-difluorothiophene, the resulting polymer pTPDPP-TF features a highly planar conjugated backbone with a high EA and IP values of -4.1 eV and -5.8 eV, respectively. A good and reversible electron-accepting ability was also observed from cyclic voltammetry. A promising n-type charge carrier mobility of 0.1 $cm^2V^{-1}s^{-1}$ was obtained in bottom-contact, top-gate OFETs. All polymer solar cells using PTB7-Th as the polymer donor gave a power-conversion efficiency of 2.72% with a high open-circuit voltage of 1.04 V. These results demonstrate that the new DPP monomer TPDPP as a potential building block for the design of n-type semiconducting polymers.

EXPERIMENTAL SECTION

Materials Thieno[2,3-*b*]pyridine[35] and 2,5-bis(trimethylstannyl)-3,4-difluorothiophene[42] were synthesized according to literature procedures. All other reagents and solvents were purchased from Sigma Aldrich, VWR, Fluorochem, Acros and used as received. Dry solvents for anhydrous reactions were purchased from Sigma Aldrich and no further attempt at drying them was made. All reactions were carried out under an inert Argon atmosphere unless otherwise stated.

Thieno[2,3-b]pyridine 7-oxide (2)

To a stirred solution of thieno[2,3-*b*]pyridine (1, 5.4 g, 40.0 mmol) in chloroform (180 mL) at room temperature, was treated with m-chloroperoxybenzoic acid (*m*-CPBA 77%, 12.4 g, 71.9

mmol) in portions over a period of 30 minutes. After the reaction mixture was stirred for over 48 hours, the solution was washed with 10% aqueous NaOH solution and then water. The organic phase was dried over $MgSO_4$, filtered and concentrated in vacuum to give a white solid (5.83 g, 96% yield). The crude product was used in the next step without any further purification. ^{1}H NMR (400 MHz, $CDCl_3$) δ 8.35 (d, *J* = 6.2 Hz, 1H), 7.77 (m, *J* = 8.0, 0.4 Hz,1H), 7.60 (d, *J* = 5.7 Hz, 1H), 7.37-7.30 (m, 2H). ^{13}C NMR (101 MHz, $CDCl_3$) δ 136.88, 134.23, 128.44, 123.08, 121.92, 121.37.

Thieno[2,3-*b*]pyridine-6-carbonitrile (3)

To a stirred solution of thieno[2,3-*b*]pyridine-7-oxide (2, 5.44 g, 36.0 mmol) in acetonitrile (360 mL) at room temperature, dimethyl carbamyl chloride (6.7 mL, 72.0 mmol) was added dropwise under argon atmosphere, followed by slowly addition of trimethyl cyanide (6.9 mL, 54.0 mmol). The reaction mixture was heated to 100 ºC. After stirred at 100 ºC for 4 hours, the reaction mixture was cooled to room temperature and then 10% K_2CO_3 aqueous solution was added to quench the reaction. The layers were allowed to separate; the organic layer is isolated and dried by $MgSO_4$, filtered, and then concentrated. The crude product was purified by column chromatography with petroleum ether/ethyl acetate (9:1) as the eluent to give compound 3 as a white solid (5.6 g, 97 % yield). ^{1}H NMR (400 MHz, $CDCl_3$) δ 8.22 (d, *J* = 8.2 Hz, 1H), 7.85 (d, *J* = 6.0 Hz, 1H), 7.70 (d, *J* = 8.2 Hz, 1H), 7.40 (d, *J* = 6.0 Hz, 1H). ^{13}C NMR (101 MHz, $CDCl_3$) δ 162.23, 134.72, 132.16, 131.54, 129.44, 123.37, 121.46, 117.55.

3,6-Bis(thieno[2,3-*b*]pyridin-6-yl)-2,5-dihydropyrrolo[3,4-*c*]pyrrole-1,4-dione (4)

Sodium (0.69 g, 30.0 mmol) and iron(III) chloride (30 mg) was added to 20 mL of 2-methyl-2-butanol and the mixture was heated to reflux until full consumption of the sodium was observed (about 3 hours). The solution was cooled to 85 ^{o}C and then thieno[2,3-*b*]pyridine-6-carbonitrile

(3, 3.2 g, 20.0 mmol) was added, followed by diethyl succinate (1.33 mL, 8.0 mmol). After stirring for 2 hours, the reaction was cooled to 50 ^{o}C, and methanol (25.0 mL) was added. The reaction was quenched by addition of glacial acetic acid (8.0 mL) and refluxed for 15 min. The reaction mixture was filtered and washed with water (2 × 50 mL), hot methanol (2 × 50 mL), acetone (2 × 25 mL) and hexane (25 mL) to afford the product as a dark purple solid (2.1 g, 52% yield), which was used without further purification.

2,5-Bis(2-octyldodecyl)-3,6-bis(thieno[2,3-*b*]pyridin-6-yl)-2,5-dihydropyrrolo[3,4-*c*]pyrrole-1,4-dione (C8C10-TPDPP)

To a mixture of 3,6-bis(thieno[2,3-b]pyridin-6-yl)-2,5-dihydropyrrolo[3,4-c]pyrrole-1,4-dione (4, 0.49 g, 1.22 mmol), potassium carbonate (0.56 g, 4.03 mmol) and 18-crown-6 (6 mg) in DMF (20 mL) was added 9-(bromomethyl)nonadecane (1.46 g, 4.03 mmol). The reaction mixture was stirred at 120 ^{o}C for overnight and then cooled to room temperature. Chloroform (50 mL) and water were added (100 mL) and the layers were separated. The organic layer was washed with saturated brine, dried over $MgSO_4$, filtered, and then concentrated in vacuum. Column chromatography on silica gel with petroleum ether/CH_2Cl_2 (4:1) as the eluent followed by recrystallization from CH_2Cl_2 and MeOH afforded C8C10-TPDPP as a deep red solid (0.35 g, 30% yield). ^{1}H NMR (400 MHz, $CDCl_3$) δ 9.10 (d, *J* = 8.5 Hz, 2H), 8.28 (d, *J* = 8.5 Hz, 2H), 7.72 (d, *J* = 6.0 Hz, 2H), 7.39 (d, *J* = 6.0 Hz, 2H), 4.46 (d, *J* = 7.2 Hz, 4H), 1.74-1.63 (m, 2H), 1.34-1.06 (m, 64H), 0.87 (dt, *J* = 8.6, 7.0 Hz, 12H). ^{13}C NMR (101 MHz, $CDCl_3$) δ 162.72, 160.92, 145.48, 144.42, 133.12, 131.51, 130.10, 123.11, 121.77, 111.66, 46.44, 38.55, 31.93, 31.89, 31.59, 30.11, 29.66, 29.57, 29.52, 29.37, 29.31, 26.56, 22.70, 14.12.

3-Bromothieno[2,3-b]pyridine-6-carbonitrile (5)

To a stirred solution of thieno[2,3-*b*]pyridine-6-carbonitrile (3, 0.32 g, 2.0 mmol) in anhydrous DMF was added N-bromosuccinimide (0.37 g, 2.1 mmol) at room temperature. The reaction mixture was stirred at room temperature for overnight. The reaction mixture was poured into water and then extracted with ethyl acetate for three times. The organic layers were collected and then washed with water and brine, dried over $MgSO_4$, filtered, and then concentrated in vacuum. Column chromatography on silica gel with petroleum ether/ethyl acetate (9:1) as the eluent gave compound 5 as a white solid (0.25 g, 53% yield). ^{1}H NMR (400 MHz, $CDCl_3$) δ 8.24 (d, J = 8.2 Hz, 1H), 7.85 (s, 1H), 7.81 (d, J = 8.2 Hz, 1H). ^{13}C NMR (101 MHz, $CDCl_3$) δ 160.36, 133.57, 131.53, 130.68, 129.13, 124.02, 117.03, 105.56.

3,6-Bis(3-bromothieno[2,3-*b*]pyridin-6-yl)-2,5-dihydropyrrolo[3,4-*c*]pyrrole-1,4-dione (6)

Sodium (86 mg, 3.75 mmol) and iron(III) chloride (3.5 mg) was added to 2.5 mL of 2-methyl-2-butanol and the mixture was heated to reflux until full consumption of the sodium was observed (about 3 hours). The solution was cooled to 85 ºC and then 3-bromothieno[2,3-*b*]pyridine-6-carbonitrile (5, 0.6 g, 2.5 mmol) was added, followed by diethyl succinate (0.17 mL, 1.0 mmol). After stirring for 2 hours, the reaction was cooled to 50 ºC, and methanol (3.0 mL) was added. The reaction was quenched by addition of glacial acetic acid (1.0 mL) and refluxed for 15 min. The reaction mixture was filtered and washed with water (2 x 20 mL), hot methanol (2 × 20 mL), acetone (2 × 10 mL) and hexane (10 mL) to afford the product 6 as a dark purple solid (0.35 g, 50% yield), which was used without further purification.

3,6-Bis(3-bromothieno[2,3-*b*]pyridin-6-yl)-2,5-bis(2-octyldodecyl)-2,5-dihydropyrrolo[3,4-*c*]pyrrole-1,4-dione (β-Br_2TPDPP)

To a mixture of 3,6-bis(3-bromothieno[2,3-*b*]pyridin-6-yl)-2,5-dihydropyrrolo[3,4-*c*]pyrrole-1,4-dione (6, 0.56 g, 1.0 mmol), potassium carbonate (0.42 g, 3.0 mmol) and 18-crown-6 (6.0 mg) in

DMF (20 mL) was added 9-(bromomethyl)nonadecane (1.31 g, 3.0 mmol). The reaction mixture was stirred at 120 ºC for overnight and then cooled to room temperature. Chloroform and water were added and the layers were separated. The organic layer was washed with saturated brine, dried over $MgSO_4$, filtered, and then concentrated in vacuum. Column chromatography on silica gel with petroleum ether/CH_2Cl_2 (4:1) as the eluent followed by recrystallization from CH_2Cl_2 and MeOH afforded β-Br_2TPDPP as a deep red solid (90 mg, 8% yield). ^{1}H NMR (400 MHz, $CDCl_3$) δ 9.18 (d, *J* = 8.5 Hz, 2H), 8.29 (d, *J* = 8.5 Hz, 2H), 7.72 (s, 2H), 4.44 (d, *J* = 7.1 Hz, 4H), 1.71-1.61 (m, 2H), 1.40-1.07 (m, 64H), 0.88 (q, *J* = 7.0 Hz, 12H).

2-Bromothieno[2,3-*b*]pyridine (7)

To a stirred solution of thieno[2,3-*b*]pyridine (1, 1.5 g, 11.1 mmol) in anhydrous THF (30 mL) was added *n*-butyllithium (2.5 M, 4.9 mL, 12.2 mmol) dropwise at -78 ºC under argon atmosphere. After the reaction mixture was stirred for one hour at -78 ºC, a solution of tetrabromomethane (4.0 g, 12.2 mmol) in anhydrous THF (10 mL) was added dropwise. After addition, the reaction mixture was allowed to warm to room temperature and then stirred for overnight. The reaction was quenched with 10% aqueous $Na_2S_2O_3$ solution and then extracted with ethyl acetate for three times. The organic phases were combined, dried over $MgSO_4$, filtered, and then concentrated. The crude product was purified by silica gel column chromatography with petroleum/ethyl acetate (4:1) as the eluent to give compound 7 as a white solid (2.23 g, 94% yield). ^{1}H NMR (400 MHz, $CDCl_3$) δ 8.60 (dd, *J* = 4.6, 1.5 Hz, 1H), 8.10 (dd, *J* = 8.0, 1.6 Hz, 1H), 7.56 (d, *J* = 6.0 Hz, 1H), 7.36-7.30 (m, 1H).

2-Bromothieno[2,3-*b*]pyridine-7-oxide (8)

To a stirred solution of 2-bromothieno[2,3-*b*]pyridine (7, 2.4 g, 11.1 mmol) in chloroform (50 mL) at room temperature, was treated with m-chloroperoxybenzoic acid (*m*-CPBA 77%, 3.11 g, 18.0

mmol) in portions over a period of 30 minutes. After the reaction mixture was stirred for over 48 hours, the solution was washed with 10% aqueous NaOH solution and then water. The organic phase was dried over $MgSO_4$, filtered and concentrated in vacuum to give a light brown solid (1.94 g, 76% yield). The crude product was used in the next step without any further purification. ^{1}H NMR (400 MHz, $CDCl_3$) δ 8.27 (dd, *J* = 6.3, 0.8 Hz, 1H), 7.63 (dd, *J* = 8.1, 0.9 Hz, 1H), 7.38 (s, 1H), 7.32 (dd, *J* = 8.1, 6.3 Hz, 1H). ^{13}C NMR (101 MHz, $CDCl_3$) δ 149.84, 136.93, 134.28, 125.64, 122.04, 120.89, 118.86.

2-Bromothieno[2,3-*b*]pyridine-6-carbonitrile (9)

To a stirred solution of 2-bromothieno[2,3-*b*]pyridine-7-oxide (8, 3.0 g, 13.04 mmol) in dichloromethane at room temperature, dimethyl carbamyl chloride (1.4 mL, 15.13 mmol) was added dropwise under argon atmosphere, followed by slowly addition of trimethyl cyanide (1.9 mL, 15.13 mmol). After the reaction mixture was stirred for 14 days at room temperature, 10% K_2CO_3 aqueous solution was added to quench the reaction. The layers were allowed to separate, the organic layer was isolated and dried by $MgSO_4$, filtered, and then concentrated. The crude product was purified by column chromatography with petroleum ether/ethyl acetate (9:1) as the eluent to give compound 9 as a white solid (1.78 g, 57% yield). ^{1}H NMR (400 MHz, $CDCl_3$) δ 8.09 (d, *J* = 8.2 Hz, 1H), 7.67 (d, *J* = 8.2 Hz, 1H), 7.44 (s, 1H).

3,6-Bis(2-bromothieno[2,3-*b*]pyridin-6-yl)-2,5-dihydropyrrolo[3,4-*c*]pyrrole-1,4-dione (10)

Sodium (0.43 g, 18.7 mmol) and iron(III) chloride (17 mg) was added to 12.5 mL of 2-methyl-2-butanol and the mixture was heated to reflux until full consumption of the sodium was observed (about 3 hours). The solution was cooled to 85 ºC and then 2-bromothieno[2,3-*b*]pyridine-6-carbonitrile 9 (3.0 g, 12.55 mmol) was added, followed by diethyl succinate (0.85 mL, 5.02 mmol). After stirring for 2 hours, the reaction was cooled to 50 ºC, and methanol (17 mL) was added. The

reaction was quenched by addition of glacial acetic acid (5 mL) and refluxed for 15 min. The reaction mixture was filtered and washed with water (2 x 50 mL), hot methanol (2 × 50 mL), acetone (2 × 25 mL) and hexane (25 mL) to afford the product as a black solid (1.4 g, 40% yield), which was used without further purification.

3,6-Bis(2-bromothieno[2,3-*b*]pyridin-6-yl)-2,5-bis(2-octyldodecyl)-2,5-dihydropyrrolo[3,4-*c*]pyrrole-1,4-dione (α-Br_2TPDPP)

To a mixture of 3,6-bis(2-bromothieno[2,3-*b*]pyridin-6-yl)-2,5-dihydropyrrolo[3,4-*c*]pyrrole-1,4-dione 10 (0.56 g, 1.0 mmol), potassium carbonate (0.42 g, 3.0 mmol) and 18-crown-6 (6 mg) in DMF (20 mL) was added 9-(bromomethyl)nonadecane (1.31 g, 3.0 mmol). The reaction mixture was stirred at 120 ^{o}C for overnight and then cooled to room temperature. Chloroform and water were added and the layers were separated. The organic layer was washed with saturated brine, dried over $MgSO_4$, filtered, and then concentrated in vacuum. Column chromatography on silica gel with petroleum ether/CH_2Cl_2 (4:1) as the eluent followed by recrystallization from CH_2Cl_2 and MeOH afforded α-Br_2TPDPP as a deep red solid (112 mg, 10% yield). ^{1}H NMR (400 MHz, $CDCl_3$) δ 9.09 (d, *J* = 8.5 Hz, 2H), 8.15 (d, *J* = 8.5 Hz, 2H), 7.42 (s, 2H), 4.41 (d, *J* = 7.3 Hz, 4H), 1.71-1.61 (m, 2H), 1.36-1.06 (m, 64H), 0.88 (q, *J* = 6.9 Hz, 12H). MS (MALDI-TOF): m/z calc for $C_{60}H_{88}Br_2N_4O_2S_2$ 1121.32; found 1121.7 (M+1).

2,5-bis(2-ethylhexyl)-3,6-bis(thieno[2,3-*b*]pyridin-6-yl)-2,5-dihydropyrrolo[3,4-*c*]pyrrole-1,4-dione (2EH-TPDPP)

To a mixture of 3,6-bis(thieno[2,3-*b*]pyridin-6-yl)-2,5-dihydropyrrolo[3,4-*c*]pyrrole-1,4-dione 4 (0.8 g, 2.0 mmol), potassium carbonate (0.91 g, 6.6 mmol) and 18-crown-6 (12 mg) in DMF (40 mL) was added 2-ethylhexyl bromide (1.2 mL, 6.6 mmol). The reaction mixture was stirred at 120 ^{o}C for overnight and then cooled to room temperature. Chloroform and water were added, and the

layers were separated. The organic layer was washed with saturated brine, dried over $MgSO_4$, filtered, and then concentrated in vacuum. Column chromatography on silica gel with petroleum ether/CH_2Cl_2 (3:1) as the eluent to afford 2EH-TPDPP as a deep red solid (0.68 g, 54% yield). ^{1}H NMR (400 MHz, $CDCl_3$) δ 9.13 (d, *J* = 8.5 Hz, 2H), 8.29 (d, *J* = 8.5 Hz, 2H), 7.72 (d, *J* = 6.0 Hz, 2H), 7.39 (d, *J* = 6.0 Hz, 2H), 4.56-4.39 (m, 4H), 1.65 (q, *J* = 6.5 Hz, 2H), 1.45-1.12 (m, 16H), 0.95-0.74 (m, 12H). ^{13}C NMR (101 MHz, $CDCl_3$) δ 162.78, 160.96, 145.47, 144.39, 133.13, 131.57, 130.16, 123.14, 121.79, 111.72, 46.19, 39.91, 30.66, 28.81, 23.96, 23.16, 14.04, 10.86.

Synthesis of pTPDPP-TF

To a microwave vial was added 3,6-Bis(2-bromothieno[2,3-*b*]pyridin-6-yl)-2,5-bis(2-octyldodecyl)-2,5-dihydropyrrolo[3,4-*c*]pyrrole-1,4-dione (α-Br_2TPDPP, 51.5 mg, 0.045 mmol, 1.0 e.q.), 2,5-bis(trimethylstannyl)-3,4-difluorothiophene (20.1 mg, 0.045 mmol, 1.0 e.q.), P(*o*Tol)$_3$ (1.23 mg, 4.05 μmol, 0.09 e.q.), $Pd_2(dba)_3$ (0.91 mg, 0.99 μmol, 0.022 e.q.). Following further degassing the microwave vial, degassed chlorobenzene (4.5 mL) was added. The microwave vial was sealed and the reaction mixture was heated at 130 ºC for 72 hours. After cooling to room temperature the reaction mixture was poured into vigorously stirring methanol and the resulting polymeric precipitate was filtered. The polymer was purified by Soxhlet extraction in a sequence of methanol, hexane, ethyl acetate, and finally chloroform. The chloroform fraction was concentrated by rotary evaporation, suspended in methanol and filtered to afford the polymer pTPDPP-TF as a dark green flake (40 mg, 82%). GPC (Chlorobenzene, 80 ºC): M_n = 24.4 kDa, M_w = 125.3 kDa, PDI = 5.1.

ASSOCIATED CONTENT

Supporting Information.

The Supporting Information is available free of charge on the ACS Publications website at DOI: Method and instruments, experimental details for fabrication and characterization of OFET and OSC devices, NMR spectra of intermediates and monomers, DSC curve of the polymer, and crystallographic data.

AUTHOR INFORMATION

Corresponding Author

*E-mail: h.chen@imperial.ac.uk (H.-Y. C.)

ACKNOWLEDGMENT

The authors thank KAUST for financial support and acknowledge EC FP7 Project SC2 (610115) EC H2020 (643791), and EPSRC Projects EP/G037515/1 and EP/M005143/1. Mingfei Xiao thanks the Cambridge Overseas Trust and Chinese Scholarship Council for PhD funding.

REFERENCES

(1) Luo, C.; Kyaw, A. K. K.; Perez, L. A.; Patel, S.; Wang, M.; Grimm, B.; Bazan, G. C.; Kramer, E. J.; Heeger, A. J. General Strategy for Self-Assembly of Highly Oriented Nanocrystalline Semiconducting Polymers with High Mobility. *Nano Lett*. **2014**, *14*, 2764–2771.

(2) Tseng, H.-R.; Phan, H.; Luo, C.; Wang, M.; Perez, L. A.; Patel, S. N.; Ying, L.; Kramer, E. J.; Nguyen, T.-Q.; Bazan, G. C.; Heeger A. J.. High-Mobility Field-Effect Transistors Fabricated with Macroscopic Aligned Semiconducting Polymers. *Adv. Mater*. **2014**, *26*,

2993–2998.

(3) Zhao, J.; Li, Y.; Yang, G.; Jiang, K.; Lin, H.; Ade, H.; Ma, W. Efficient Organic Solar Cells Processed From Hydrocarbon Solvents. *Nat. Energy* **2016**, *1*, 15027.

(4) Yao, H.; Ye, L.; Zhang, H.; Li, S.; Zhang, S.; Hou, J. Molecular Design of Benzodithiophene-Based Organic Photovoltaic Materials. *Chem. Rev.* **2016**, *116*, 7397–7457.

(5) Sun, B.; Hong, W.; Yan, Z.; Aziz, H.; Li, Y. Record High Electron Mobility of 6.3 $cm^2V^{-1}s^{-1}$ Achieved for Polymer Semiconductors Using a New Building Block. *Adv. Mater.* **2014**, *26*, 2636–2642.

(6) Bucella, S. G.; Luzio, A.; Gann, E.; Thomsen, L.; McNeill, C. R.; Pace, G.; Perinot, A.; Chen, Z.; Facchetti, A.; Caironi, M. Macroscopic and High-Throughput Printing of Aligned Nanostructured Polymer Semiconductors for MHz Large-Area Electronics. *Nat. Commun.* **2015**, *6*, 8394.

(7) Hwang, Y.-J.; Courtright, B. A. E.; Ferreira, A. S.; Tolbert, S. H.; Jenekhe, S. A. 7.7% Efficient All-Polymer Solar Cells. *Adv. Mater.* **2015**, *27*, 4578–4584.

(8) Li, Z.; Xu, X.; Zhang, W.; Meng, X.; Ma, W.; Yartsev, A.; Inganäs, O.; Andersson, M. R.; Janssen, R. A. J.; Wang, E. High Performance All-Polymer Solar Cells by Synergistic Effects of Fine-Tuned Crystallinity and Solvent Annealing. *J. Am. Chem. Soc.* **2016**, *138*, 10935–10944.

(9) Ye, L.; Jiao, X.; Zhao, W.; Zhang, S.; Yao, H.; Li, S.; Ade, H.; Hou, J. Manipulation of Domain Purity and Orientational Ordering in High Performance All-Polymer Solar Cells. *Chem. Mater.* **2016**, *28*, 6178–6185.

(10) Gao, L.; Zhang, Z.-G.; Xue, L.; Min, J.; Zhang, J.; Wei, Z.; Li, Y. All-Polymer Solar Cells Based on Absorption-Complementary Polymer Donor and Acceptor with High Power Conversion Efficiency of 8.27%. *Adv. Mater.* **2016**, *28*, 1884–1890.

(11) Guo, Y.; Li, Y.; Awartani, O.; Han, H.; Zhao, J. Improved Performance of All-Polymer Solar Cells Enabled by Naphthodiperylenetetraimide-Based Polymer Acceptor. *Adv. Mater.* **2017**, *29*, 1700309.

(12) Zhan, X.; Tan, Z.; Domercq, B.; An, Z.; Zhang, X.; Barlow, S.; Li, Y.; Zhu, D.; Kippelen, B.; Marder, S. R. A High-Mobility Electron-Transport Polymer with Broad Absorption and Its Use in Field-Effect Transistors and All-Polymer Solar Cells. *J. Am. Chem. Soc.* **2007**,

129, 7246–7247.

(13) Zhou, E.; Cong, J.; Wei, Q.; Tajima, K.; Yang, C.; Hashimoto, K. All-Polymer Solar Cells From Perylene Diimide Based Copolymers: Material Design and Phase Separation Control. *Angew. Chem. Int. Ed.* **2011**, *50*, 2799–2803.

(14) Zhou, E.; Cong, J.; Hashimoto, K.; Tajima, K. Control of Miscibility and Aggregation via the Material Design and Coating Process for High-Performance Polymer Blend Solar Cells. *Adv. Mater.* **2013**, *25*, 6991–6996.

(15) Zhou, E.; Nakano, M.; Izawa, S.; Cong, J.; Osaka, I.; Takimiya, K.; Tajima, K. All-Polymer Solar Cell with High Near-Infrared Response Based on a Naphthodithiophene Diimide (NDTI) Copolymer. *ACS Macro Lett.* **2014**, *3*, 872–875.

(16) Yang, J.; Xiao, B.; Tajima, K.; Nakano, M.; Takimiya, K. Comparison Among Perylene Diimide (PDI), Naphthalene Diimide (NDI), and Naphthodithiophene Diimide (NDTI) Based N-Type Polymers for All-Polymer Solar Cells. *Macromolecules* **2017**, *50*, 3179–3185.

(17) Tang, A.; Zhan, C.; Yao, J.; Zhou, E. Design of Diketopyrrolopyrrole (DPP)-Based Small Molecules for Organic-Solar-Cell Applications. *Adv. Mater.* **2017**, *29*, 1600013.

(18) Nielsen, C. B.; Turbiez, M.; McCulloch, I. Recent Advances in the Development of Semiconducting DPP-Containing Polymers for Transistor Applications. *Adv. Mater.* **2013**, *25*, 1859–1880.

(19) Vezie, M. S.; Few, S.; Meager, I.; Pieridou, G.; Dörling, B.; Ashraf, R. S.; Goni, A. R.; Bronstein, H.; McCulloch, I.; Hayes, S. C.; *et al*. Exploring the Origin of High Optical Absorption in Conjugated Polymers. *Nat. Mater.* **2016**, *15*, 746.

(20) Ashraf, R. S.; Meager, I.; Nikolka, M.; Kirkus, M.; Planells, M.; Schroeder, B. C.; Holliday, S.; Hurhangee, M.; Nielsen, C. B.; Sirringhaus, H.; *et al*. Chalcogenophene Comonomer Comparison in Small Band Gap Diketopyrrolopyrrole-Based Conjugated Polymers for High-Performing Field-Effect Transistors and Organic Solar Cells. *J. Am. Chem. Soc.* **2015**, *137*, 1314–1321.

(21) Venkateshvaran, D.; Nikolka, M.; Sadhanala, A.; Lemaur, V.; Zelazny, M.; Kepa, M.; Hurhangee, M.; Kronemeijer, A. J.; Pecunia, V.; Nasrallah, I.; *et al*. Approaching Disorder-Free Transport in High-Mobility Conjugated Polymers. *Nature* **2014**, *515*, 384–388.

(22) Choi, H.; Ko, S.-J.; Kim, T.; Morin, P.-O.; Walker, B.; Lee, B. H.; Leclerc, M.; Kim, J. Y.;

Heeger, A. J. Small-Bandgap Polymer Solar Cells with Unprecedented Short-Circuit Current Density and High Fill Factor. *Adv. Mater.* **2015**, *27*, 3318–3324.

(23) Zhou, E.; Cong, J.; Hashimoto, K.; Tajima, K. Introduction of a Conjugated Side Chain as an Effective Approach to Improving Donor–Acceptor Photovoltaic Polymers. *Energy Environ. Sci.* **2012**, *5*, 9756–9759.

(24) Grzybowski, M.; Gryko, D. T. Diketopyrrolopyrroles: Synthesis, Reactivity, and Optical Properties. *Adv. Optical Mater.* **2015**, *3*, 280–320.

(25) Bronstein, H.; Chen, Z.; Ashraf, R. S.; Zhang, W.; Du, J.; Durrant, J. R.; Tuladhar, P. S.; Song, K.; Watkins, S. E.; Geerts, Y.; *et al*. Thieno[3,2-B]Thiophene-Diketopyrrolopyrrole-Containing Polymers for High-Performance Organic Field-Effect Transistors and Organic Photovoltaic Devices. *J. Am. Chem. Soc.* **2011**, *133*, 3272–3275.

(26) Li, Y.; Sonar, P.; Murphy, L.; Hong, W. High Mobility Diketopyrrolopyrrole (DPP)-Based Organic Semiconductor Materials for Organic Thin Film Transistors and Photovoltaics. *Energy Environ. Sci.* **2013**, *6*, 1684–1710.

(27) Sonar, P.; Singh, S. P.; Li, Y.; Soh, M. S.; Dodabalapur, A. A Low-Bandgap Diketopyrrolopyrrole-Benzothiadiazole-Based Copolymer for High-Mobility Ambipolar Organic Thin-Film Transistors. *Adv. Mater.* **2010**, *22*, 5409–5413.

(28) Park, J. H.; Jung, E. H.; Jung, J. W.; Jo, W. H. A Fluorinated Phenylene Unit as a Building Block for High-Performance N-Type Semiconducting Polymer. *Adv. Mater.* **2013**, *25*, 2583–2588.

(29) Yun, H.-J.; Kang, S. J.; Xu, Y.; Kim, S. O.; Kim, Y.-H.; Noh, Y.-Y.; Kwon, S.-K. Dramatic Inversion of Charge Polarity in Diketopyrrolopyrrole-Based Organic Field-Effect Transistors via a Simple Nitrile Group Substitution. *Adv. Mater.* **2014**, *26*, 7300–7307.

(30) Li, W.; Roelofs, W. S. C.; Turbiez, M.; Wienk, M. M.; Janssen, R. A. J. Polymer Solar Cells with Diketopyrrolopyrrole Conjugated Polymers as the Electron Donor and Electron Acceptor. *Adv. Mater.* **2014**, *26*, 3304–3309.

(31) Li, W.; An, Y.; Wienk, M. M.; Janssen, R. A. J. Polymer–Polymer Solar Cells with a Near-Infrared Spectral Response. *J. Mater. Chem. A* **2015**, *3*, 6756–6760.

(32) Li, Y.; Sonar, P.; Singh, S. P.; Soh, M. S.; van Meurs, M.; Tan, J. Annealing-Free High-Mobility Diketopyrrolopyrrole-Quaterthiophene Copolymer for Solution-Processed Organic Thin Film Transistors. *J. Am. Chem. Soc.* **2011**, *133*, 2198–2204.

(33) Bronstein, H.; Collado-Fregoso, E.; Hadipour, A.; Soon, Y. W.; Huang, Z.; Dimitrov, S. D.; Ashraf, R. S.; Rand, B. P.; Watkins, S. E.; Tuladhar, P. S.; Meager I.; Durrant J. R.; McCulloch I. Thieno[3,2-*b*]Thiophene-Diketopyrrolopyrrole Containing Polymers for Inverted Solar Cells Devices with High Short Circuit Currents. *Adv. Funct. Mater.* **2013**, *23*, 5647–5654.

(34) Meager, I.; Ashraf, R. S.; Mollinger, S.; Schroeder, B. C.; Bronstein, H.; Beatrup, D.; Vezie, M. S.; Kirchartz, T.; Salleo, A.; Nelson, J.; McCulloch I. Photocurrent Enhancement from Diketopyrrolopyrrole Polymer Solar Cells Through Alkyl-Chain Branching Point Manipulation. *J. Am. Chem. Soc.* **2013**, *135*, 11537–11540.

(35) Jia, H.; Dai, G.; Weng, J.; Zhang, Z.; Wang, Q.; Zhou, F.; Jiao, L.; Cui, Y.; Ren, Y.; Fan, S.; Zhou J.; Qing W.; Gu Y.; Wang J.; Sai Y.; Su W. Discovery of (*S*)-1-(1-(Imidazo[1,2-*a*]Pyridin-6-yl)Ethyl)-6-(1-Methyl-1 H-Pyrazol-4-yl)-1*H*-[1,2,3]Triazolo[4,5-*b*]Pyrazine (Volitinib) as a Highly Potent and Selective Mesenchymal–Epithelial Transition Factor (c-Met) Inhibitor in Clinical Development for Treatment of Cancer. *J. Med. Chem.* **2014**, *57*, 7577–7589.

(36) Qi, T.; Guo, Y.; Liu, Y.; Xi, H.; Zhang, H.; Gao, X.; Liu, Y.; Lu, K.; Du, C.; Yu, G.; Zhu D. Synthesis and Properties of the *anti* and *syn* Isomers of Dibenzothieno[*b*, *d*]Pyrrole. *Chem. Commun.* **2008**, 6227–6229.

(37) Mueller, C. J.; Singh, C. R.; Fried, M.; Huettner, S.; Thelakkat, M. High Bulk Electron Mobility Diketopyrrolopyrrole Copolymers with Perfluorothiophene. *Adv. Funct. Mater.* **2015**, *25*, 2725–2736.

(38) Li, Y.; Sonar, P.; Singh, S. P.; Zeng, W.; Soh, M. S. 3,6-Di(furan-2-yl)Pyrrolo[3,4-*c*]Pyrrole-1,4(2*H*,5*H*)-Dione and Bithiophene Copolymer with Rather Disordered Chain Orientation Showing High Mobility in Organic Thin Film Transistors. *J. Mater. Chem.* **2011**, *21*, 10829–10835.

(39) Yue, W.; Nikolka, M.; Xiao, M.; Sadhanala, A.; Nielsen, C. B.; White, A. J. P.; Chen, H.-Y.; Onwubiko, A.; Sirringhaus, H.; McCulloch, I. Azaisoindigo Conjugated Polymers for High Performance N-Type and Ambipolar Thin Film Transistor Applications. *J. Mater. Chem. C* **2016**, *4*, 9704–9710.

(40) Zhang, S.; Ye, L.; Zhao, W.; Liu, D.; Yao, H.; Hou, J. Side Chain Selection for Designing Highly Efficient Photovoltaic Polymers with 2D-Conjugated Structure. *Macromolecules*

2014, *47*, 4653–4659.

(41) Stoltzfus, D. M.; Donaghey, J. E.; Armin, A.; Shaw, P. E.; Burn, P. L.; Meredith, P. Charge Generation Pathways in Organic Solar Cells: Assessing the Contribution from the Electron Acceptor. *Chem. Rev.* **2016**, *116*, 12920–12955.

(42) Sakamoto, Y.; Komatsu, S.; Suzuki, T. Tetradecafluorosexithiophene: the First Perfluorinated Oligothiophene. *J. Am. Chem. Soc.* **2001**, *123*, 4643–4644.

Table of Contents